JACS
JOURNAL OF THE AMERICAN CHEMICAL SOCIETY
Article
pubs.acs.org/JACS

Spin Accommodation and Reactivity of Silver Clusters with Oxygen: The Enhanced Stability of Ag_{13}^-

Zhixun Luo,[†] Gabriel U. Gamboa,[‡] Jordan C. Smith,[†] Arthur C. Reber,[‡] J. Ulises Reveles,[‡] Shiv N. Khanna,*[,‡] and A. W. Castleman, Jr.*[,†,§]

[†]Department of Chemistry, The Pennsylvania State University, University Park, Pennsylvania 16802, United States
[‡]Department of Physics, Virginia Commonwealth University, Richmond, Virginia 23284, United States
[§]Department of Physics, The Pennsylvania State University, University Park, Pennsylvania 16802, United States

Supporting Information

ABSTRACT: Spin accommodation is demonstrated to play a determining role in the reactivity of silver cluster anions with oxygen. Odd-electron silver clusters are found to be especially reactive, while the anionic 13-atom cluster exhibits unexpected stability against reactivity with oxygen. Theoretical studies show that the odd−even selective behavior is correlated with the excitation needed to activate the O−O bond in O_2. Furthermore, by comparison with the reactivity of proximate even-electron clusters, we demonstrate that the inactivity of Ag_{13}^- is associated with its large spin excitation energy, ascribed to a crystal-field-like splitting of the orbitals caused by the bilayer atomic structure, which induces a large gap despite not having a magic number of valence electrons.

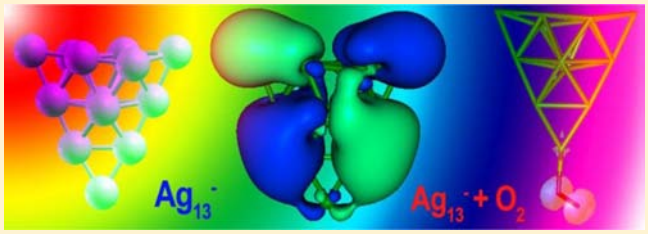

INTRODUCTION

Bulk silver is a shiny noble metal widely used in jewelry, silverware, and welding. Silver is susceptible to strong oxidizers and is used in the development of photographic film. When exposed to the atmosphere, the metal can be corroded in humid environments (by H_2S and other sulfites, chlorates, and HCl, to form Ag_2S and AgCl). In addition to the bulk, silver particles also exhibit unique optical, electrical, and thermal properties and have found applications in photovoltaics, antibacterial coatings, chemical sensors, and so on.[1] This wide range of applications has inspired extensive studies on small silver clusters and, in particular, the oxidation and catalytic properties of small clusters containing two to a few dozen atoms.[2−13] Recently Klacar et al.[11] examined the reactivity of Ag_n ($n \leq 9$) clusters with O_2 within a density functional theory (DFT) scheme and showed that dissociation of the molecular oxygen could be preferred on larger-sized clusters while molecular adsorption was favored for $n \leq 5$. Bernhardt et al.[10] measured the energies for binding of O_2 to small silver anion clusters. Studies by Hagen et al.[13] observed cooperative effects in the binding of multiple O_2 molecules to even-electron clusters, while single molecules preferred to bind to odd-electron clusters. Furthermore, the even-atom cluster anions (i.e., clusters having an odd number of valence electrons) were found to be more reactive than the odd-atom cluster anions for the reaction of the first O_2. Socaciu et al.[12] investigated the reactivity of anionic silver clusters Ag_n^- containing 1−11 atoms with O_2 and found some unusual trends. Their results showed that Ag_n^- (n = 1−11) clusters react readily with molecular oxygen to generate $Ag_nO_2^-$ products for clusters containing an even number of silver atoms, (Ag_4^- was found to bind three O_2 molecules), while the clusters containing an odd number of silver atoms (except n = 1) react to bind two O_2 molecules.

It is well-known that molecular oxygen is a spin triplet in its ground state and that the two half-filled molecular orbitals are antibonding in nature. The cleavage of an O−O bond requires the filling of the half-filled antibonding orbitals in $^3O_2$, and this process reduces the multiplicity of the molecule from triplet to singlet.[14] However, silver and oxygen are expected to have negligible spin−orbit effects, and hence, their reaction should follow the Wigner−Witmer rules of spin conservation (i.e., the reaction should conserve the overall spin of the system).[14−16] For silver anion clusters with an odd number of electrons (i.e., Ag_{2n}^-), the spin of the cluster can be aligned opposite to that of the $^3O_2$ molecule, allowing a spin-conserved pathway to the final product (eq 1).

$$^2Ag_{2n}^- + {}^3O_2 \rightarrow {}^2[Ag_{2n}O_2]^- \rightarrow {}^2Ag_{2n}O_2^- \quad (1)$$

However, silver cluster anions with an even number of electrons (i.e., Ag_{2n+1}^-) require a spin excitation of the remaining portion to conserve the total spin (eq 2).[13]

$$^1Ag_{2n+1}^- + {}^3O_2 \rightarrow {}^3[Ag_{2n+1}O_2]^- \xrightarrow{\text{spin crossing}} {}^1Ag_{2n+1}O_2^- \quad (2)$$

In these equations, the ground states of the Ag clusters have the lowest spin multiplicity (singlet for even-electron clusters and

Received: April 4, 2012
Published: October 31, 2012

   dx.doi.org/10.1021/ja303268w | J. Am. Chem. Soc. 2012, 134, 18973−18978

doublet for odd-electron clusters). It is notable that for clusters with an even number of electrons, two-state reactivity[15] may be hypothesized to play a role, as it allows intersystem crossings from one spin channel to another; however, the spin conservation of Al-based clusters reacting with oxygen has been unambiguously confirmed.[14,16] Experimental studies of the reactivity of oxygen with Ag_n^- clusters have been performed on smaller-sized clusters, but clusters with $11 < n < 20$ remain to be further explored.

It is worth mentioning that because oxygen is a strong etchant, stable clusters can be identified via their resistance to etching. For example, Al_{13}^-, $Al_{13}I_{2n}^-$, $Al_{14}I_3^-$, Al_7C^-, and $Al_4H_7^-$ have previously been identified as stable clusters that are resistant to etching by oxygen, and their enhanced stability has been linked to the spin excitation energy.[17−32] Among these magic clusters, the number 13 has attracted extensive interest, and several other classes of metal clusters have also been found to exhibit similar stability, such as Au_{13}^- and Pd_{13}^-.[33,34] It would be interesting to ascertain whether similar principles can be applicable to silver clusters. A silver atom has a filled 4d shell with a single electron in the 5s orbital. The electronic behavior of silver clusters, including the progression of the geometry with size, is often rationalized within a confined nearly free electron gas (NFEG) model developed originally for alkali atom clusters. The Ag_{13}^- cluster contains 14 valence electrons and does not correspond to a filled shell in the confined NFEG as modeled in the spherical jellium model,[35] for which the superatomic electronic shells exhibit an ordering $1S^2\ 1P^6\ 1D^{10}\ 2S^2\ 1F^{14}\ 2P^6$ .... (We denote delocalized orbitals with upper-case letters and atomic orbitals with lower-case letters.)

In this work, by employing a magnetron sputtering (MagS) cluster source, we undertook a synergistic study combining experiments on the reactivity of silver cluster anions with oxygen and first-principles DFT calculations to examine the atomic and electronic structures of Ag_n^- clusters containing up to 20 silver atoms and their reactivity with oxygen. As shown below, the experimental studies indicated that Ag clusters with an even number of electrons exhibit lower reactivity than those with an odd number of electrons. More importantly, Ag_{13}^- was identified as a stable species that is resistant to etching by oxygen. It is notable that 13-atom clusters generally have compact geometric shapes,[36] leading to a jellium grouping of states; however, 14 is not a magic number of electrons, so one would expect Ag_{13}^- to react with O_2. The size-selective resistance to oxidation of Ag_{13}^- is due to its large HOMO−LUMO gap and large spin excitation energy. The unexpectedly large HOMO−LUMO gap for Ag_{13}^- with 14 valence electrons is due to its bilayer structure, which opens a large gap via a crystal-field splitting of the delocalized 1D orbitals.[37] Such investigations further the understanding of mechanisms involved in cluster reactivity.

EXPERIMENTAL AND THEORETICAL METHODS

High-purity helium (Praxair, Inc., purity >99.995%), ultrahigh-purity argon (Praxair, Inc., purity >99.99%), and high-purity oxygen (Praxair, Inc., 99.99%) were used. The silver disk (99.99% pure, 50 mm diameter, 6 mm thickness) was obtained from Kurt J. Lesker Company. The reactions leading to the current findings were carried out in a previously described apparatus that uses a MagS cluster source to provide a tunable size distribution of silver clusters.[38,39] A DC power supply (TDK-Lambda Americas Inc., Genesys 750 W/1500 W) was used to provide the high voltages needed for the MagS source. High-purity helium was introduced from the inlet at the rear of the magnetron chamber to carry the clusters through an adjustable iris into a flow tube, where they encountered and reacted with O_2 at room temperature. The oxygen gas was introduced to the cluster beam ∼30 cm downstream from the source and allowed to react with the Ag clusters over a 60 cm distance and a time of ∼8 ms. The pressure in the reaction flow tube was kept at 0.7 Torr, that is, the number of collisions for the clusters and reactant could be up to 100.[18] The products were then extracted into a differentially pumped ion-guide vacuum system and analyzed with a quadrupole mass spectrometer (Extrel QMS).

To investigate the mechanism of oxidation and the origin of the reactivity in these species, we carried out theoretical investigations of the ground-state geometries and electronic properties of neutral Ag_n and anionic Ag_n^- clusters containing up to 17 Ag atoms. We also studied the binding energy of O_2 to selected Ag_n^- clusters ($n = 1−17$) to probe the nature of the bonding and the spin-transfer effects. A first-principles molecular orbital approach was used wherein the cluster wave function was expressed as a linear combination of atomic orbitals centered at the atomic sites and the exchange−correlation effects were included within a generalized gradient approximation (GGA) DFT formalism. The actual calculations were carried out using the deMon2k set of computer codes.[40] For the exchange and correlation functionals, we used the Perdew−Burke−Ernzerhof (PBE) GGA functional.[41] The silver atoms were described using a 19-electron quasi-relativistic effective core potential (QECP) with a corresponding valence basis set as proposed by Andrae et al.,[41] while the DZVP-GGA basis set[42] was used for the oxygen atoms. The auxiliary density was expressed as a combination of primitive Hermite Gaussian functions by using the GEN-A2* auxiliary function set.[43] To determine the geometries and spin multiplicities of the ground states, the configuration space was sampled by starting from several initial configurations and spin multiplicities and then optimizing the geometric structures via the quasi-Newton Levenberg−Marquardt method.[44] To allow for full variational freedom, all of the structures were fully optimized in delocalized redundant coordinates without imposing any symmetry constraints.

RESULTS AND DISCUSSION

Figure 1a presents the mass spectrum of Ag_n^- clusters, and Figure 1b−e shows the mass intensity of the reacted species after the clusters were exposed to different quantities of oxygen. Figure 1a shows that the unreacted species exhibited a nearly normal distribution of sizes with a broad maximum at clusters containing 13−15 atoms. The distribution of sizes changed dramatically upon reaction with oxygen (Figure 1b−e). These experimental findings show three distinct features: (i) clusters containing an even number of Ag atoms (odd number of valence electrons) showed a decrease in intensity upon reaction, with the simultaneous formation of $Ag_nO_2^-$ products; (ii) clusters containing an odd number of Ag atoms demonstrated reduced reactivity toward oxygen, except for Ag_{15}^-, for which a clear $Ag_{15}O_2^-$ peak was observed; and (iii) Ag_{13}^- appeared as a magic species in the mass spectra of the reacted species. Figure 1e shows that at an oxygen flow rate of 18 sccm, Ag_{13}^- was the only pure silver cluster with significant intensity, proving that it is the Ag_n^- cluster with the lowest reactivity toward O_2 among clusters with $n = 9−17$. Figure 1c,d shows the spectra at intermediate flow rates of 4 and 7 sccm, in which more oxides of the Ag_n^- clusters were observed, including a weak peak for $Ag_{13}O_2^-$. It is notable that Figure 1d,e shows substantial intensity of $Ag_2O_2^-$, which provides evidence that some clusters were etched down to smaller sizes, although in the case of $Ag_2O_2^-$, the other products in this reaction were neutralized and undetectable in the mass spectra. Such an etching effect resembles the fragmentation of aluminum clusters upon reaction with oxygen.[14,16] The observation of $Ag_2O_2^-$ is also in accordance with the results

dx.doi.org/10.1021/ja303268w | J. Am. Chem. Soc. 2012, 134, 18973−18978

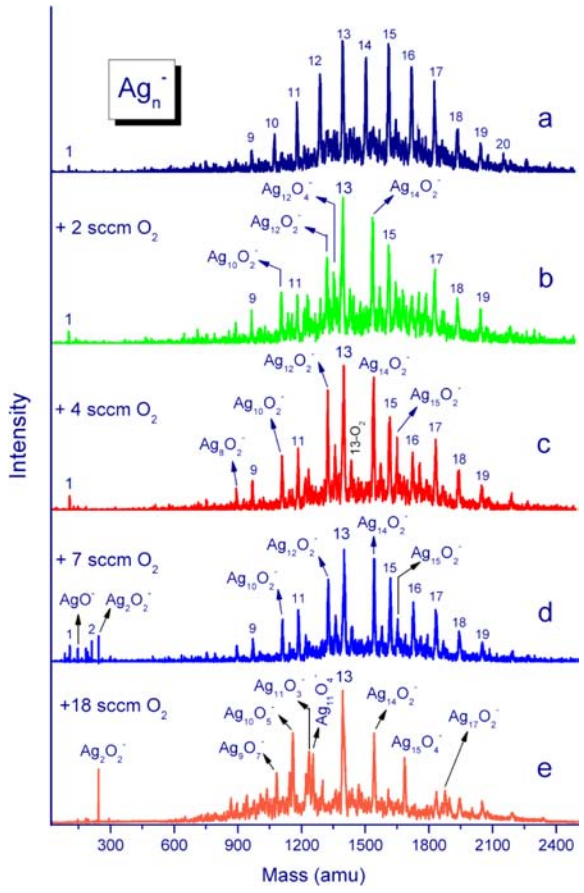

Figure 1. Mass spectra of (a) silver cluster anions produced via a MagS source and (b) after exposure to different quantities of oxygen.

of previous studies of charge-state-dependent adsorption behavior of O_2 on silver dimers.[45]

To compare the reactivities of these silver clusters, Figure 2 displays the integrated intensities for Ag_{11}^-, Ag_{12}^-, Ag_{13}^-, Ag_{14}^-

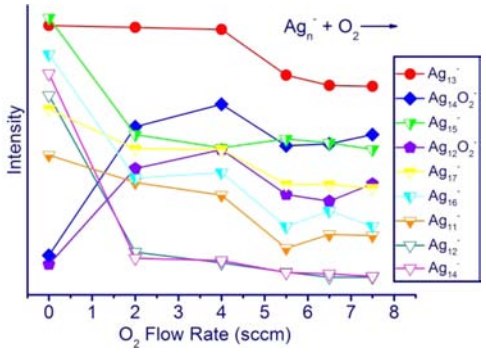

Figure 2. Integrated intensities of Ag_{11}^-, Ag_{12}^-, Ag_{13}^-, Ag_{14}^-, Ag_{15}^-, Ag_{16}^-, Ag_{17}^-, $Ag_{12}O_2^-$, and $Ag_{14}O_2^-$ as functions of oxygen flow rate (0–8 sccm). The points represent the data and the lines are drawn only to aid the reader.

Ag_{15}^-, Ag_{16}^-, Ag_{17}^-, $Ag_{12}O_2^-$, and $Ag_{14}O_2^-$ as functions of oxygen flow rate. Ag_{12}^- and Ag_{14}^- react strongly even at a flow rate of 2 sccm, while Ag_{13}^- is most abundant even at the highest concentration of O_2 (Figure 1e). Among the even-electron cluster anions, Ag_{15}^- and Ag_{17}^- are more reactive than Ag_{13}^- and show mild reactivity even at low oxygen rates. Moreover, Ag_{13}^- remains a magic species with a different size distribution of initial clusters as shown in Figure S3 in the Supporting Information. The intensities of $Ag_{12}O_2^-$ and $Ag_{14}O_2^-$ were not observed to increase linearly with the quantity of oxygen, in part because of successive reactions with O_2 to produce $Ag_{12}O_4^-$ and $Ag_{14}O_4^-$, respectively.[45] Furthermore, the larger clusters may be etched down to form smaller clusters at high oxygen flow rates.[17]

Figure 3 shows the ground-state geometries of silver cluster anions containing up to 17 atoms. The Ag clusters with $n \leq 6$

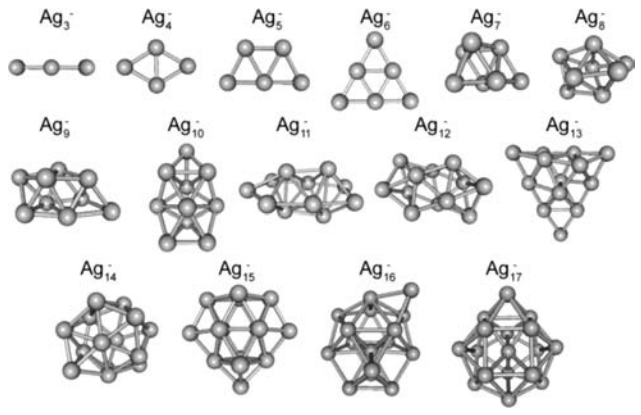

Figure 3. Ground-state structures of Ag_n^- clusters ($n \leq 17$) obtained via DFT with a gradient-corrected functional.

exhibit a quasi-planar structure, while those with $n > 6$ display three-dimensional structures. A similar progression from quasi-planar to compact structures also occurs in alkali-metal clusters and can be rationalized within the confined NFEG model in terms of initial filling of the 1S, $1P_x$, and $1P_y$ orbitals to make planar structures that become compact upon filling of the $1P_z$ orbitals. The ground state of Ag_6^- is planar with regular triangular symmetry. In comparison with its isomer having a tetrahedral Ag_4^- core and two faces decorated with Ag atoms, the planar Ag_6^- cluster was found to be 0.06 eV lower in energy. Ag_7^- is a square bipyramid with one face decorated with a Ag atom. Further addition of Ag atoms leads to compact structures until $n = 13$, where Ag_{13}^- was found to present a bilayer structure instead of the compact icosahedral structure exhibited by many metallic clusters (e.g., Al_{13}). The bilayer structure of Ag_{13}^- is reminiscent of a similar structure recently identified as the ground state of Pd_{13} and is different from the ground state of Au_{13}^-, which is a planar structure.[33] The ground state of Ag_{13}^- is followed by close-lying isomers (for more details of the geometries and relative stabilities of the isomers of Ag_{13}^-, see Figure S4 in the Supporting Information). Further addition of Ag to Ag_{13}^- (to form larger species) results in more compact species. The calculated structures of Ag_n^- are almost the same as those reported previously, except for Ag_{12}^-, for which we found a slightly lower energy structure.[46−48]

To examine the energetic stability of Ag_n^- clusters, we calculated the incremental binding energy (IBE), that is, the energy gain as a Ag atom is added to a certain cluster, defined as

$$\mathrm{IBE} = E(\mathrm{Ag}^0) + E(\mathrm{Ag}_{n-1}^-) - E(\mathrm{Ag}_n^-) \quad (3)$$

where $E(Ag^0)$, $E(Ag_{n-1}^-)$, and $E(Ag_n^-)$ are the total energies of a Ag atom and cluster anions containing $n - 1$ and n Ag atoms, respectively. The IBEs are displayed as the red symbols in Figure 4A. An even/odd oscillation is evident, with the even-

dx.doi.org/10.1021/ja303268w | J. Am. Chem. Soc. 2012, 134, 18973−18978

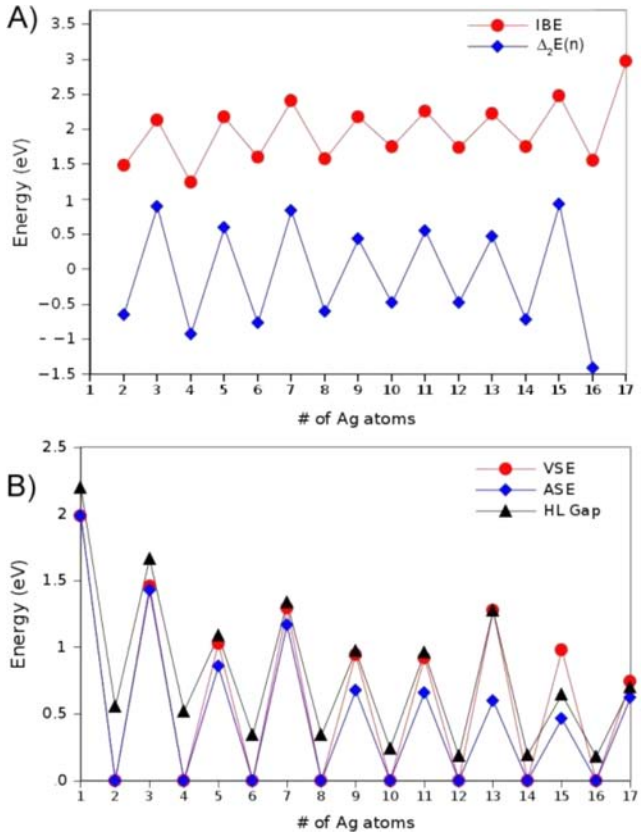

Figure 4. (A) Calculated incremental binding energies (red ●) and second energy differences (blue ◆) of the Ag_n^- clusters; (B) vertical spin excitation energies (red ●), adiabatic spin excitation energies (blue ◆), and HOMO−LUMO gaps (black ▲) of the Ag_n^- clusters. The lines are drawn as guides to the eye.

electron Ag_n^- clusters exhibiting higher IBEs than the odd-electron clusters. This pattern is due to the enhanced stability of clusters with fully occupied orbitals.

To examine further any magic clusters, we also calculated the second difference in energy (Δ_2E), defined as

$$\Delta_2E(n) = E(Ag_{n-1}^-) + E(Ag_{n+1}^-) - 2E(Ag_n^-) \quad (4)$$

These values are shown as the blue symbols in Figure 4A. Other than the even/odd pattern, $\Delta_2E(n)$ also shows no distinctive peaks. In particular, the IBE and Δ_2E of Ag_{13}^- are similar to those of the other odd-atom silver cluster anions. What then makes Ag_{13}^- a magic species in the reaction of Ag_n^- with oxygen?

Furthermore, we compared three classes of calculated values: (1) the HOMO−LUMO energy gap; (2) the vertical spin excitation energy (VSE), which is the lowest energy required to excite the cluster (Ag_{2n+1}^-) from the original singlet state to the triplet state with no geometry rearrangement; and (3) the adiabatic spin excitation energy (ASE), which represents the energy difference between the ground state of the anion (singlet) and the triplet state with relaxed geometry rearrangement. The odd-electron species (Ag_{2n}^-) were treated as having no spin excitation (i.e., both the VSE and ASE were set equal to 0) because $Ag_{2n}O_2^-$ can have the same spin multiplicity as the original bare cluster Ag_{2n}^-, eliminating the need for spin excitation. In contrast, the clusters with an even number of electrons (Ag_{2n+1}^-) may show variable reactivity that correlates with the VSE. The results are shown in Figure 4B, where the red, blue, and black symbols show the VSE, ASE, and HOMO−LUMO gap, respectively. The strong even/odd effects in both the HOMO−LUMO gap and the spin excitation energies are evident. Ag_{13}^- has the highest VSE and HOMO−LUMO gap among the Ag_n^- clusters with $8 \le n \le 17$, and the large spin excitation energy is responsible for its reduced reactivity and enhanced stability.

For cluster anions with n = 2−17, we also calculated the adiabatic electron detachment energy (DE), defined as DE = $E_{total}(Ag_n^-) - E_{total}(Ag_n^0)$, and found that the DE of Ag_{13}^- is larger than those for all of the other clusters ($n \le 16$), as shown in Figure 5, where a comparison with previously reported

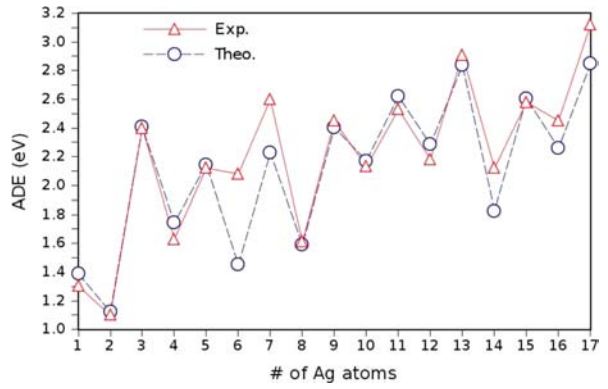

Figure 5. Calculated adiabatic electron detachment energies (△) and experimental[49] detachment energies (○) of Ag_n^- cluster anions. The lines are drawn to guide the eye.

experimental results is displayed. It is notable that except for Ag_6^-, which lies on the threshold of transition from a two-dimensional to a three-dimensional structure, all of the values from the literature accord very well with our theoretical results.[49−51]

Figure 6 presents the calculated energies for binding of the oxygen molecule to the anionic silver clusters, in which the O−O bond remains intact. The oxygen binding energies exhibit a strong even−odd alternation, with the values for $Ag_{2n}O_2^-$ being consistently higher than those of the adjacent $Ag_{2n+1}O_2^-$. An

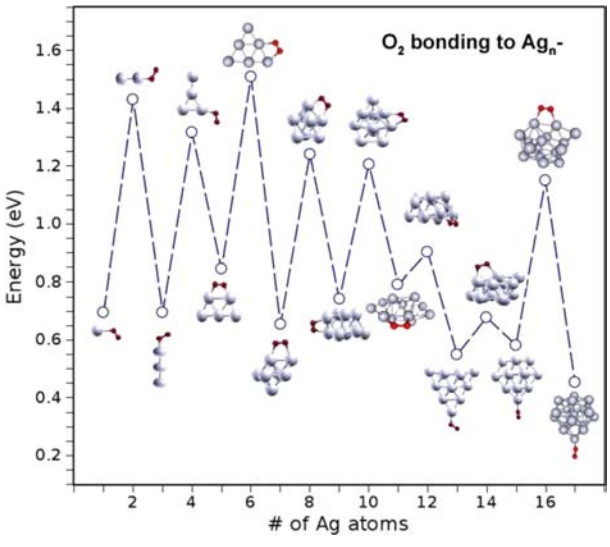

Figure 6. Energies for binding of O_2 to Ag_n^-. The dashed line is drawn to guide the eye.

dx.doi.org/10.1021/ja303268w | J. Am. Chem. Soc. 2012, 134, 18973−18978

overall decrease in O_2 binding energy was found for larger cluster sizes of even-electron clusters. However, $Ag_{13}O_2^-$ showed the second-lowest O_2 binding energy (lower than that of $Ag_{15}O_2^-$). It is worth mentioning that the calculated binding energies are larger than those measured in experiments,[10] probably as a result of a delocalization error that results in overbinding of O_2. The O_2 binding energies to Ag_n^- (n = 2−5) were experimentally estimated in ref 10 to be 1.64, 0.37, 1.23, and 0.57 eV, compared with our calculated values of 1.43, 0.69, 1.32, and 0.84 eV, respectively. It should be noted that the calculated values show the same trend as the experimental ones.

To demonstrate the role of spin in the reactivity of O_2 with Ag clusters, we performed theoretical investigations on the binding of an O_2 molecule to Ag_{13}^-. Figure 7a shows the

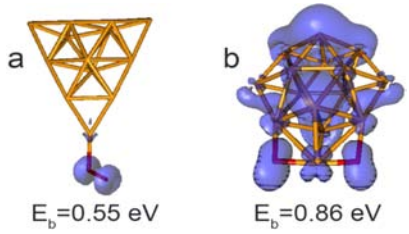

Figure 7. (a) Optimized geometry and electronic spin density of $^3[Ag_{13}O_2]^-$, obtained by taking the difference between the spin-up and spin-down charge densities; (b) geometry of $Ag_{15}O_2^-$, in which oxygen is completely inserted into the silver cluster. The atoms and bonds are displayed as tube models (Ag, gold; O, red).

optimized geometry and spin density of the resulting complex, obtained by taking the difference between the spin-up and spin-down charge densities. Also given is the net binding energy (BE) of the O_2 molecule to the cluster, calculated as

$$\mathrm{BE} = E(^3O_2) + E(^1Ag_{13}^-) - E(^3[Ag_{13}O_2]^-) \quad (5)$$

It should be noted that the energy required to excite an O_2 molecule from the triplet state to the singlet state is 0.98 eV.[52] Figure 7a shows that the spin is localized on the O_2 molecule, which is ascribed to the relatively large spin excitation energy (VSE = 1.28 eV). This also lowers the energy for binding of the O_2 molecule to the cluster. To confirm this further, we also examined the reaction of Ag_{13}^- with singlet O_2. However, it was found that the O−O bond broke and the O atoms were inserted into the cluster. This means that the observed stability of Ag_{13}^- in the reaction with O_2 is related to its large spin excitation energy (1.28 eV).

For comparison, we also considered Ag_{15}^-, which is reactive despite having an even number of electrons. The VSE of Ag_{15}^- is 0.65 eV, versus 1.28 eV for Ag_{13}^-. To examine the reaction, we brought an O_2 molecule toward the cluster while optimizing the geometry by moving atoms in the direction of the interaction force (Figure 7b). After optimization, the oxygen was completely inserted into the silver cluster, with no O−O bond remaining. This is the same as the result seen for the odd-electron systems (Ag_{2n}^-), where the spin excitation energies are negligible.[14] The spin transfer results in the filling of the antibonding orbitals, and hence, the activated oxygen reacts readily with minimal energetic cost for insertion into the cluster.

The Ag_{13}^- cluster has a large HOMO−LUMO gap, even though it has 14 valence electrons, which do not correspond to a filled electronic shell within the spherical jellium model.[35] Figure 8 shows the molecular orbitals in the cluster. The

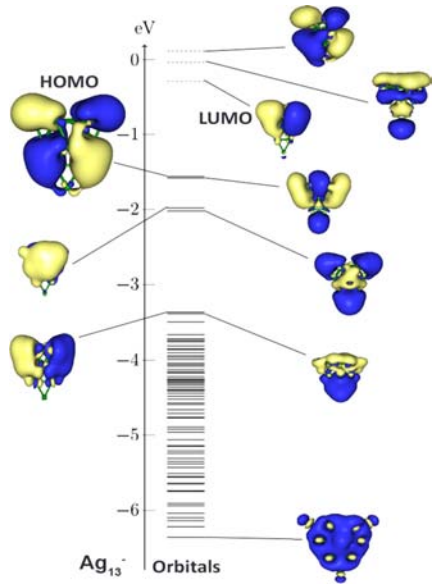

Figure 8. Calculated molecular orbitals for Ag_{13}^-.

electronic states below −3.3 eV are mostly composed of Ag 4d states that can be regarded as core states. Following the core sequence are a set of delocalized orbitals spread throughout the cluster. The delocalized NFEG orbitals are best described as $1S^2 \mid 1P^4 \mid 1P^2\ 2S^2 \mid 1D^4 \parallel 1D^6$, where the single vertical lines indicate observed gaps and the double vertical line indicates the gap between the filled and unfilled orbitals. The splitting of $1P^6$ and $1D^{10}$ into separate subshells demonstrates that the spherical jellium model does not describe the electronic structure of Ag_{13}^-. The geometric distortion of the cluster to a bilayer structure results in a splitting of these orbitals that can be viewed as the crystal-field splitting of the D orbitals.[37] In the present case, two of the 1D orbitals in the plane of the bilayer structure are stabilized while three are unfilled, leading to a large crystal-field splitting at the subfilling of the D shell. Consequently, the quasi-inert behavior of Ag_{13}^- is rooted in its bilayer structure that leads to a crystal-field splitting of the D manifold, resulting in a large HOMO−LUMO gap and electron detachment energy.

■ CONCLUSIONS

We have shown that the variation in the reactivity of silver cluster anions with oxygen and the unusual magic nature of Ag_{13}^- are associated with the spin excitations needed to activate the O−O bond in O_2. The clusters with an even number of Ag atoms (odd numbers of electrons) are quite reactive, as such clusters and the product after reaction with O_2 can have the same spin. Clusters with an odd number of Ag atoms (even number of electrons), however, require a spin accommodation (as the antibonding orbitals of the O_2 are filled) to activate/break the O−O bond. The reactivity of these Ag_n^- clusters is related to the spin excitation energy, and clusters with low spin excitation energy bind O_2 strongly and are more reactive. Finally, clusters such as Ag_{13}^- have high spin excitation energy and are not observably reactive. Here, the high spin excitation energy results from a distortion in geometry that leads to a splitting of the D shell, leading to a large electron detachment

dx.doi.org/10.1021/ja303268w | J. Am. Chem. Soc. 2012, 134, 18973−18978

energy and HOMO−LUMO gap at a subshell level. The present studies demonstrate how spin conservation, the ability of clusters to accommodate spin excitation, and the modification of electronic shells via geometrical distortions can account for the observed variable reactivity of silver clusters with oxygen.

■ ASSOCIATED CONTENT

Supporting Information

Schematics of the experimental setup and the MagS source, data for different size distributions, and the isomers of Ag_{13}^-. This material is available free of charge via the Internet at http://pubs.acs.org.

■ AUTHOR INFORMATION

Corresponding Author

snkhanna@vcu.edu; awc@psu.edu

Notes

The authors declare no competing financial interest.

■ ACKNOWLEDGMENTS

We thank Dr. W. Hunter Woodward for his consultation. This material is based upon work supported by the Air Force Office of Science Research under AFOSR Award FA9550-10-1-0071 (Z.L., J.C.S., A.W.C.) and through MURI Grant FA9550-08-1-0400 (G.U.G., A.C.R., J.U.R., S.N.K.).

■ REFERENCES

(1) Walter, R. C. *Gold and Silver*; Wiley: New York, 1908; pp 496−649.
(2) Fenske, D.; Persau, C.; Dehnen, S.; Anson, C. E. *Angew. Chem., Int. Ed.* **2004**, *43*, 305−309.
(3) Rao, T. U. B.; Pradeep, T. *Angew. Chem., Int. Ed.* **2010**, *49*, 3925−3929.
(4) Carroll, S. J.; Seeger, K.; Palmer, R. E. *Appl. Phys. Lett.* **1998**, *72*, 305−307.
(5) Harb, M.; Rabilloud, F.; Simon, D.; Rydlo, A.; Lecoultre, S.; Conus, F.; Rodrigues, V.; Felix, C. *J. Chem. Phys.* **2008**, *129*, No. 194108.
(6) Yang, X.; Cai, W.; Shao, X. *J. Phys. Chem. A* **2007**, *111*, 5048−5056.
(7) Janata, E. *J. Phys. Chem. B* **2003**, *107*, 7334−7336.
(8) Ye, G. X.; Michely, T.; Weidenhof, V.; Friedrich, I.; Wuttig, M. *Phys. Rev. Lett.* **1998**, *81*, 622−625.
(9) Bernhardt, T. M. *Int. J. Mass Spectrom.* **2005**, *243*, 1−29.
(10) Bernhardt, T. M.; Hagen, J.; Lang, S. M.; Popolan, D. M.; Socaciu-Siebert, L. D.; Wöste, L. *J. Phys. Chem. A* **2009**, *113*, 2724−2733.
(11) Klacar, S.; Hellman, A.; Panas, I.; Grönbeck, H. *J. Phys. Chem. C* **2010**, *114*, 12610−12617.
(12) Socaciu, L. D.; Hagen, J.; Le Roux, J.; Popolan, D.; Bernhardt, T. M.; Woste, L.; Vajda, S. *J. Chem. Phys.* **2004**, *120*, 2078−2081.
(13) Hagen, J.; Socaciu, L. D.; Le Roux, J.; Popolan, D.; Bernhardt, T. M.; Wöste, L.; Mitrić, R.; Noack, H.; Bonačić-Koutecký, V. *J. Am. Chem. Soc.* **2004**, *126*, 3442−3343.
(14) Reber, A. C.; Khanna, S. N.; Roach, P. J.; Woodward, W. H.; Castleman, A. W., Jr. *J. Am. Chem. Soc.* **2007**, *129*, 16098−16101.
(15) Schwarz, H. *Int. J. Mass Spectrom.* **2004**, *237*, 75−105.
(16) Burgert, R.; Schnoeckel, H.; Grubisic, A.; Li, X.; Stokes, S. T.; Bowen, K. H.; Ganteför, G. F.; Kiran, B.; Jena, P. *Science* **2008**, *319*, 438−442.
(17) Li, X.; Grubisic, A.; Stokes, S. T.; Cordes, J.; Gantefor, G. F.; Bowen, K. H.; Kiran, B.; Willis, M.; Jena, P.; Burgert, R.; Schnokel, H. *Science* **2006**, *315*, 356−358.
(18) Leuchtner, R. E.; Harms, A. C.; Castleman, A. W., Jr. *J. Chem. Phys.* **1989**, *91*, 2753−2754.
(19) Khanna, S. N.; Jena, P. *Phys. Rev. Lett.* **1992**, *69*, 1664−1667.
(20) Baruah, T.; Pederson, M. R.; Zope, R. J.; Beltran, M. R. *Chem. Phys. Lett.* **2004**, *387*, 476−480.
(21) Bergeron, D. E.; Castleman, A. W., Jr.; Morisato, T.; Khanna, S. N. *Science* **2004**, *304*, 84−87.
(22) Bergeron, D. E.; Roach, P. J.; Castleman, A. W., Jr.; Jones, N. O.; Khanna, S. N. *Science* **2005**, *307*, 231−235.
(23) Reveles, J. U.; Khanna, S. N.; Roach, P. J.; Castleman, A. W., Jr. *Proc. Natl. Acad. Sci. U.S.A.* **2006**, *103*, 18405−18410.
(24) Kawamata, H.; Negishi, Y.; Nakajima, A.; Kaya, K. *Chem. Phys. Lett.* **2001**, *337*, 255−262.
(25) Koyasu, K.; Atobe, J.; Akutsu, M.; Mitsui, M.; Nakajima, A. *J. Phys. Chem. A* **2007**, *111*, 42−49.
(26) Reber, A. C.; Khanna, S. N.; Castleman, A. W., Jr. *J. Am. Chem. Soc.* **2007**, *129*, 10189−10194.
(27) Leskiw, B. D.; Castleman, A. W., Jr. *Chem. Phys. Lett.* **2000**, *316*, 31−36.
(28) Khanna, S. N.; Jena, P. *Phys. Rev. B* **1995**, *51*, 13705−13716.
(29) Reveles, J. U.; Clayborne, P. A.; Reber, A. C.; Khanna, S. N.; Pradhan, K.; Sen, P.; Pederson, M. R. *Nat. Chem.* **2009**, *1*, 310−315.
(30) Roach, P. J.; Reber, A. C.; Woodward, W. H.; Khanna, S. N.; Castleman, A. W., Jr. *Proc. Natl. Acad. Sci. U.S.A.* **2007**, *104*, 14565−14569.
(31) Castleman, A. W., Jr. *J. Phys. Chem. Lett.* **2011**, *2*, 1062−1069.
(32) Castleman, A. W., Jr.; Khanna, S. N. *J. Phys. Chem. C* **2009**, *113*, 2664−2675.
(33) Gruber, M.; Heimel, G.; Romaner, L.; Brédas, J.-L.; Zojer, E. *Phys. Rev. B* **2008**, *77*, No. 165411.
(34) Köster, A. M.; Calaminici, P.; Orgaz, E.; Roy, D. R.; Reveles, J. U.; Khanna, S. N. *J. Am. Chem. Soc.* **2011**, *133*, 12192−12196.
(35) Knight, W. D.; Clemenger, K.; de Heer, W. A.; Saunder, W. A.; Chou, M. Y.; Cohen, M. L. *Phys. Rev. Lett.* **1984**, *52*, 2141−2144.
(36) Piotrowski, M. J.; Piquini, P.; Da Silva, J. F. L. *Phys. Rev B* **2010**, *81*, No. 155446.
(37) Roach, P. J.; Woodward, W. H.; Reber, A. C.; Khanna, S. N.; Castleman, A. W., Jr. *Phys. Rev. B* **2010**, *81*, No. 195404.
(38) Luo, Z.; Smith, J. C.; Woodward, W. H.; Castleman, A. W., Jr. *J. Phys. Chem. A* **2012**, *116*, 2012−2017.
(39) Luo, Z.; Woodward, W. H.; Smith, J. C.; Castleman, A. W., Jr. *Int. J. Mass Spectrom.* **2011**, *309*, 176−181.
(40) Köster, A. M.; Geudtner, G.; Calaminici, P.; Casida, M. E.; Dominguez, V. D.; Flores-Moreno, R.; Gamboa, G. U.; Goursot, A.; Heine, T.; Ipatov, A.; Janetzko, F.; del Campo, J. M.; Reveles, J. U.; Vela, A.; Zuniga-Gutierrez, B.; Salahub, D. R. *deMon2k*, version 3; The deMon Developers: Cinvestav, Mexico City, 2011.
(41) Perdew, J. P.; Burke, K.; Ernzerhof, M. *Phys. Rev. Lett.* **1996**, *77*, 3865−3868.
(42) Andrae, D.; Häußermann, U.; Dolg, M.; Stoll, H.; Preuß, H. *Theor. Chim. Acta* **1990**, *77*, 123−141.
(43) Calaminici, P.; Janetzko, F.; Köster, A. M.; Mejia-Olvera, R.; Zuniga-Gutierrez, B. *J. Chem. Phys.* **2007**, *126*, No. 044108.
(44) Reveles, J. U.; Köster, A. M. *J. Comput. Chem.* **2004**, *25*, 1109−1116.
(45) Socaciu, L. D.; Hagen, J.; Heiz, U.; Bernhardt, T. M.; Leisner, T.; Wöste, L. *Chem. Phys. Lett.* **2001**, *340*, 282−288.
(46) Fernández, E. M.; Soler, J. M.; Garzón, I. L.; Balbás, L. C. *Phys. Rev. B* **2004**, *70*, No. 165403.
(47) Bonačić-Koutecký, V.; Ĉešpiva, L.; Fantucci, P.; Pittner, J.; Koutecký, K. *J. Chem. Phys.* **1994**, *100*, 490−506.
(48) Zhang, H.; Tian, D. *Comput. Mater. Sci.* **2008**, *42*, 462−469.
(49) Handschuh, H.; Chia-Yen, C.; Bechthold, P. S.; Ganterför, G.; Eberhardt, W. *J. Chem. Phys.* **1995**, *102*, 6406−6422.
(50) Ganteför, G.; Gausa, M.; Meiwes-Broer, K.-H.; Lutz, H. O. *J. Chem. Soc., Faraday Trans.* **1990**, *86*, 2483−2488.
(51) Alameddin, G.; Hunter, J.; Cameron, D.; Kappes, M. M. *Chem. Phys. Lett.* **1992**, *192*, 122−128.
(52) Carsky, P.; Hubac, I. *Int. J. Quantum Chem.* **2002**, *90*, 1031−1037.